THE JOURNAL OF PHYSICAL CHEMISTRY B

Article

pubs.acs.org/JPCB

Dynamics of Discotic Fluoroalkylated Triphenylene Molecules Studied by Proton NMR Relaxometry

Fabián Vaca Chávez,*[,†] Pedro J. Sebastião,[†,‡] Yasuo Miyake,[§] Hirosato Monobe,[§] and Yo Shimizu[§]

[†]Condensed Matter Physics Centre, University of Lisbon, Lisbon, Portugal

[‡]Departamento de Física, Instituto Superior Técnico, Technical University of Lisbon, Lisbon, Portugal

[§]National Institute of Advanced Industrial Science and Technology, Kansai Center, 1-8-31 Midorigaoka, Ikeda, Osaka 563-8577, Japan

Supporting Information

ABSTRACT: The Larmor frequency and temperature dependence of the proton nuclear magnetic resonance (NMR) spin−lattice relaxation time was measured in the isotropic and columnar phases of both chain-end fluorinated triphenylene disk-like and fully hydrogenated molecules. In the columnar phase, the results are interpreted in terms of the collective motions, due to the deformations of the columns, and individual molecular translational self-diffusion displacements and rotations/reorientacions. In the isotropic phase, local molecular motions and order fluctuations as a pretransitional effect were considered. The activation energies of the molecular motions of the partially fluorinated molecule were found to be higher than those corresponding to the hydrocarbon homologue. Our findings show a clear difference in the relaxation dispersion between the two liquid crystals homologues. In particular it is observed that the columnar undulations have a much stronger contribution to the relaxation rate in the low frequency regime in the case of the fully hydrogenated triphenylene. The effect of fluorination of the pheripheral chain enhances the columnar mesophase's stability.

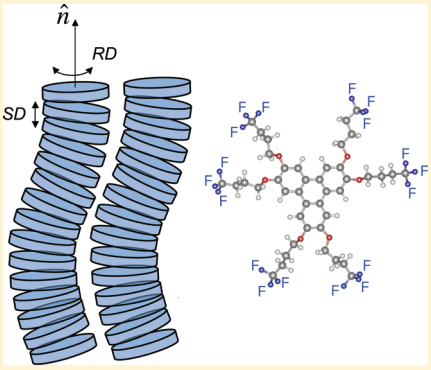

INTRODUCTION

Due to their order in the columnar mesophase,[1,2] discotic liquid crystallyne compounds are suitable for a vast field of applications in materials science and molecular electronics. The π-orbitals of adjacent molecules overlap and yield a one-dimensional pathway for charge migration along the column.[3−5] This offers promising possibilities for application of these materials in photocopying and nanoscale molecular electronic devices like light-emitting diodes, field-effect transistors,[6,7] and photovoltaic cells.[8−14]

The key issues to obtain a material with high charge mobility include the degree of homeotropic alignment of the columnar structure, the degree of order within the column, the size and the electronic overlap's extent of the $\pi-\pi$ conjugated system in the aromatic core.[15,16]

Since the discovery of triphenylene as a molecular core for the design of discotic liquid crystals,[2] the physical and structural properties of some derivatives have been widely studied in detail.[17−19] Recently, it was found that a strong tendency toward homeotropic alignment of the hexagonal columnar (Col_h) mesophase is obtained by introducing a perfluoroalkyl group into the peripheral chains of triphenylene mesogens.[20,21] It was also revealed that the introduction of perfluoroalkyl parts into the peripheral chains tends to enhance the thermal stability of the columnar mesophase. It was observed that the columnar phase is disordered even for the C4 chain length,[21] while the corresponding hydrocarbon chain derivative exhibits hexagonal plastic mesophase.[22] This modification provides an additional method for the reinforcement of molecular alignment and molecular packing control in a Col_h mesophase.

Due to the importance of the molecular alignment control and the stability of the columns, it is essential to obtain a detailed description of the molecular motion within the columns. To this end, it is well-known that nuclear magnetic resonance (NMR) is a powerful experimental tool, widely used in vast areas of research and applied, in particular, to study the molecular dynamics of liquid crystals.[23] NMR has been extensively used for investigations of the molecular order, structure, and dynamics in columnar mesophases formed by different disk-like molecules. Žumer and Vilfan developed a model for the nuclear spin relaxation of disk-like molecules in the liquid crystalline phases.[24] This model was used on the study of the molecular dynamics of hexapentoxy-triphenylene by Vilfan et al.[25] by measuring the proton self-diffusion coefficient and spin−lattice relaxation in the laboratory (T_1) and in the rotating frame ($T_{1\rho}$). ^{2}H NMR studies on selectively deuterated samples included the measurement of quadrupolar splitting (ν_Q), two-dimensional (2D) exchange spectroscopy, and spin−lattice (T_{1Z} and T_{1Q}) and spin−spin (T_2) relaxation times.[26−33] Also, the ring and aliphatic chains carbons order parameters and magic angle spinning (MAS) NMR carbon-13 measurements were reported.[34−36]

Received: July 1, 2011
Revised: January 30, 2012
Published: February 22, 2012

dx.doi.org/10.1021/jp206225t | J. Phys. Chem. B 2012, 116, 2339−2346

A complementary and well-established technique to study the molecular dynamics is the measurement of the Larmor frequency dependence of NMR spin−lattice relaxation time T_1 (NMRD), for a broad frequency range from kilohertz to a few hundred megahertz (typically up to 300 MHz for ^{1}H). This method provides the possibility to obtain detailed information about molecular motions.[37] Individual molecular motions, such as translational diffusion and anisotropic rotational processes of single molecules, can be distinguished from the peculiar molecular dynamics feature of liquid crystalline mesophases, namely, collective molecular reorientations.[38]

^{1}H NMRD profiles in the isotropic and columnar phases of fully protonated disk-like molecules with triphenylene core were measured previously showing that the NMR measurements are sensitive to elastic deformation of the columns, strengthening the fact that this is a suitable technique to study dynamics of such compounds.[39,40]

In the case of calamitic liquid crystals, the presence of fluoroalkyl groups in the molecules enhances the mesophase thermal stability and increases the facility of appearing of smectic phases.[41,42]

The effect of fluorine on the molecular dynamics of partially fluorinated disk-like molecules in the columnar phase was studied by Dong et al.[43] By measuring the temperature dependence of ν_Q, T_{1Z}, and T_{1Q}, at two different Larmor frequencies, on a ring-deuterated 1-fluoro-2,3,6,7,10,11-hexahexyloxytriphenylene (F-HAT6), they found an increase in the stability of the columns. Dahn et al.[44] reported a decrease of the clearing point of triphenylene substituted with only one partially fluorinated side chain, but nonessential changes in the mesophase were shown.

Here, the results of the spin−lattice relaxation time measured over more than four decades of Larmor frequency of 2,3,6,7,10,11-hexakis-(1*H*,1*H*,2*H*,2*H*,3*H*,3*H*-perfluorobutyloxy)-triphenylene (F1C4 from now on) discotic liquid crystal in the Col_h and isotropic phases are presented. The molecule consists on a protonated triphenylene core and aliphatic chains except the CH_3 groups that were replaced by CF_3 as schematically represented in Figure 1. The results are compared with those obtained for the corresponding hydrocarbon homologue (C1C4).

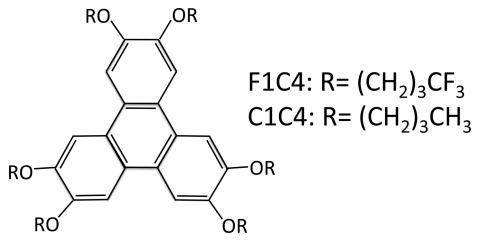

Figure 1. Molecular structure of the disk-like fully protonated and partially fluorinated triphenylene molecules.

EXPERIMENTAL SECTION

Samples. The liquid crystals studied here were synthesized according to the method described by Terasawa et al.[21] The phase transitions temperatures were determined by differential scanning calorimetry (DSC), and under cooling, the following sequences were found:

$$\text{F1C4:}\quad \text{Iso} \xrightarrow{171\,^\circ\text{C}} \text{Col}_h \xrightarrow{132\,^\circ\text{C}} \text{Cr}$$

$$\text{C1C4:}\quad \text{Iso} \xrightarrow{143\,^\circ\text{C}} \text{Col}_h \xrightarrow{78\,^\circ\text{C}} \text{Col}_x \xrightarrow{44\,^\circ\text{C}} \text{Cr}$$

The Col_x phase detected for the C1C4 is probably a highly ordered columnar mesophase. Samples of the two compounds were sealed in standard 5 mm NMR tubes under vacuum.

NMR Measurements. The proton spin−lattice relaxation rate, $R_1(\equiv 1/T_1)$, was measured over more than four Larmor frequency, $\nu_L = \omega/2\pi$, decades, from 10 kHz to 300 MHz. In the range 10 kHz−8.9 MHz, the data were obtained with a home-developed fast field-cycling (FFC) relaxometer[45] operating with a polarization and detection fields of 0.215 T and a switching time less than 3 ms. For frequencies between 10 and 91 MHz, a variable-field iron-core magnet and a Bruker Avance II console were used. At 300 MHz, a Bruker Avance II spectrometer was used. R_1 was measured applying the inversion recovery $(\pi)_x - \tau - (\pi/2)_{x,-x} -$ Acq sequence in the case of the standard NMR spectrometers.

Prior to all R_1 measurements, the samples were heated up to around 10 °C above the Col_h−Iso transition temperature in the presence of the static magnetic field where they remained around 40 min for stabilization. All R_1 measurements were performed after slow cooling, rate of 1 °C/min, to the desired temperature. The temperature was regulated and stabilized to within ±0.5 °C using gas flow.

RESULTS AND DISCUSSIONS

Columnar Phase. Proton R_1 dispersion curves were obtained for the columnar mesophase F1C4 at 165, 150, and 135 °C and at 132, 110, and 88 °C for C1C4. The results corresponding to the highest and lowest temperatures for each sample are shown in the Figure 2. The remaining results are

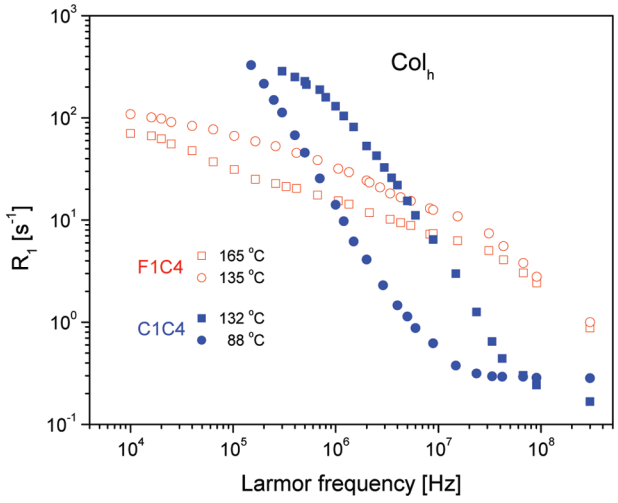

Figure 2. R_1 vs Larmor frequency in the Col_h phase at two temperatures for each sample.

presented in the Supporting Information. The first remark that we can immediately make from the data is the obvious difference in the values of R_1 in the whole measurements frequency range and the different shape of the spin−lattice relaxation dispersion profiles. Although the relaxation mechanisms present in the Col_h of both compounds are expected to be the same, the differences may come from their dissimilar relative contributions.

In addition, the temperature dependence of R_1 was measured at different Larmor frequencies: 15.5 MHz and 40 kHz for F1C4 and 14.83, 8.9, and 1 MHz for C1C4. Some results are displayed in Figure 3, and the others can be found in the Supporting Information. Two relaxation rates R_1 were obtained

dx.doi.org/10.1021/jp206225t | J. Phys. Chem. B 2012, 116, 2339−2346

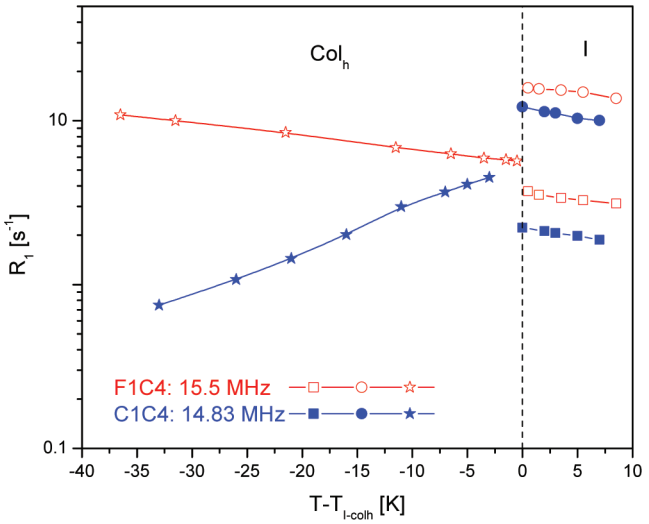

Figure 3. R_1 vs temperature in the Col$_h$ and isotropic phases at 15.5 and 14.83 MHz for F1C4 and C1C4, respectively. The behavior is similar for both compounds in the isotropic phase but completely different in the Col$_h$. The solid lines are a guide for the eyes.

in the isotropic phase (vide infra), and an abrupt change takes place at the temperature corresponding to the Iso−Col$_h$ transition, showing only a monoexponential magnetization decay in the Col$_h$ phase. While a quite similar behavior is found in the isotropic phase of both compounds, a noticeable difference in the Col$_h$ phase is observed.

In order to analyze the data, we make use of the well-established models associated with the different relaxation mechanisms expected to be present in the Col$_h$ phase. The onset of columnar order induces significant changes in molecular mobility, and column deformations have to be considered as an important relaxation mechanism.

In the Col$_h$ phase of disk-like molecules, we assumed that the following mechanisms contribute to the proton relaxation:

(i) While *order director fluctuations* are the collective motions of rodlike molecules in the nematic and smectic-A mesophases, *elastic column deformations* (ECD) are the collective motions that affect the spin−lattice relaxation in the case of discotic molecules in the Col$_h$ phase. This type of motion was first referred to by Levelut[46] and later by Žumer and Vilfan.[24] The proposed relaxation mechanism considers the spectral density:

$$J_{ECD}(\omega) = \frac{kT\eta}{2\pi^2} \times \int_{q_{\perp,low}}^{q_{\perp,high}} \int_{q_{\parallel,low}}^{q_{\parallel,high}} \frac{q_\perp \, dq_\perp q_\parallel^{\,4} \, dq_\parallel}{\omega^2\eta^2 q_\parallel^{\,4} + (K_3 q_\parallel^{\,4} + B q_\perp^{\,2})^2}$$

B and K_3 are the elastic constants for bending and compression of the columns, respectively. η is the effective viscosity. $q_{\perp,high}$ and $q_{\parallel,high}$ are the components of the largest wave vectors of the deformation parallel and perpendicular to the columns, respectively. The shortest wave vectors are $q_{\perp,low}$ and $q_{\parallel,low}$. High and low cutoff frequencies can be defined in terms of the limit wave vectors and the viscoelastic constants.[24] Power series in temperature were considered for the strength of ECD and for the cutoff frequencies.

(ii) Rotational reorientations of the alkyl chains of the molecule modulate mainly the intramolecular proton interaction. This motion is here described by a BBP type[47] function with a orientational correlation time τ_{Rot} which is assumed to possess an Arrhenius like temperature dependence, $\tau_{Rot}(T) = \tau_{r,\infty} \exp(E_r/RT)$. E_r is the activation energy, and R is the universal gas constant.

(iii) Translational diffusion of the molecules (SD) is either intracolumnar motion or an intercolumnar permeation. The corresponding relaxation rate was previously calculated.[24] The mathematical expression of the relaxation rate for the rotational diffusions $R_{1,SD}$ is an integral function that may be approximated by a BPP type curve. The prefactor (see eq 2) is related to the spin density, n, and translational diffusion jump distance, d. Here, the corresponding correlation time is also assumed thermally activated, as $\tau_{SD}(T) = \tau_{SD,\infty} \exp(E_{SD}/RT)$.

(iv) Due to the moment of inertia of the disk-like molecules around their symmetry axis, it is expected that associated rotations are much slower than the rotational reorientation of the alkyl chains and contribute to the relaxation with a different correlation time. The relaxation rate for the rotational diffusions is $R_{1,RD}$, and it is here also described by a BBP type function.

A schematic representation of some molecular motions present in the Col$_h$ phase is displayed in Figure 4.

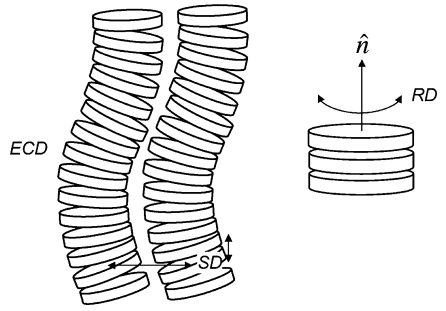

Figure 4. Schematic representation of the molecular motions in the Col$_h$ phase. See text for details.

As it is commonly considered for liquid crystalline systems, the total experimental R_1 is the sum of different contributions, as

$$R_1 = R_{1,ECD} + R_{1,Rot} + R_{1,SD} + R_{1,RD} \quad (1)$$

Here we assume that each contribution is statistically independent of the others.

The BPP model used is in the form:[47]

$$R_{1,i} = A_i \left[\frac{\tau_i}{1 + (\omega\tau_i)^2} + \frac{4\tau_i}{1 + (2\omega\tau_i)^2} \right]$$
$$i = \text{Rot, SD, RD} \quad (2)$$

where A_i reflects the dipolar interaction strength and τ_i is the correlation time.

With the proposed models, a simultaneous model fit of the frequency and temperature dependence of R_1 was performed using a nonlinear least-squares minimization procedure.[48] The results of the main model fitting parameters are listed in Table 1. Figure 5 shows the experimental data, presented in Figure 2, and the corresponding theoretical fitting curves of R_1 of the NMRD profiles together with the different contributions to the

dx.doi.org/10.1021/jp206225t | J. Phys. Chem. B 2012, 116, 2339−2346

Table 1. Details of the Fitting Parameters According to the Proposed Models to Describe the Frequency and Temperature Dependence of R_1 in the Col_h Phase of C1C4 and F1C4

mechanism	parameter	F1C4	C1C4
SD	$\tau_{SD,\infty}$ [s]	1.6×10^{-15}	3.9×10^{-13}
	E_{SD} [kJ/mol]	60	32
	A_{SD} [s^{-2}]	8.3×10^{7}	5.6×10^{6}
Rot	$\tau_{r,\infty}$ [s]	1.8×10^{-16}	1.7×10^{-14}
	E_r [kJ/mol]	49	15.3
	A_{Rot} [s^{-2}]	1.3×10^{9}	2.1×10^{10}
RD	$\tau_{RD,\infty}$ [s]	9.9×10^{-15}	
	E_{RD} [kJ/mol]	43	
	A_{RD} [s^{-2}]	7.1×10^{8}	

total fitting curves. As it is observed, the proposed models describe very well the experimental data. The rotational reorientation of the chains (Rot) is the dominant mechanism at high frequencies while the self-diffusion and the rotational diffusion around the columnar axis (in the case of F1C4) are more relevant at intermediate frequencies.

It is expected that the collective motions ECD dominate the sub-megahertz range. This is the case for F1C4, but this relaxation mechanism is effective in a much wider frequency range for C1C4 (up to ~30 MHz at the highest measured temperature) meaning that the columns formed by the fully protonated disk-like molecules undulate with larger wavelengths. Figure 6 confirms this analysis as the R_1 temperature dependence observed at frequencies around 15 MHz is quite different in both systems. The fit of the temperature dependence of R_1 at 15.5 MHz for F1C4 and 14.83 MHz for C1C4 in the Col_h phase with the contributions to the total relaxation rate from the different mechanisms is shown.

The strength of $R_{1,SD}$ (A_{SD}) depends on n and d, both assumed to be temperature independent.[24] The estimated values for the two compounds are $n_{C1C4} = 5.47 \times 10^{28}$ m^{-3} and $n_{F1C4} = 2.56 \times 10^{28}$ m^{-3}. From the fitting parameter A_{SD}, a value $d = 5.7$ Å was obtained for F1C4 and 19 Å for C1C4. These values are close to the intracolumnar and intercolumnar molecular distances, respectively. The intercolumnar diffusion relaxation mechanism is more effective in the protonated disk-like molecules than the intercolumnar mechanism. Here, our results show that in the case of F1C4 it is the opposite. For this process we obtained the values $\tau_{SD} = 77$ ns at 135 °C and 23 ns at 165 °C for the mean time between intracolumnar jumps for F1C4. These values are longer than $\tau_{SD} = 5.2$ ns at 132 °C and 16 ns at 88 °C obtained for C1C4. The later agrees with the ~10 ns obtained for the intercolumnar jump in similar fully protonated systems by Vilfan et al. for hexapentoxy-triphenylene

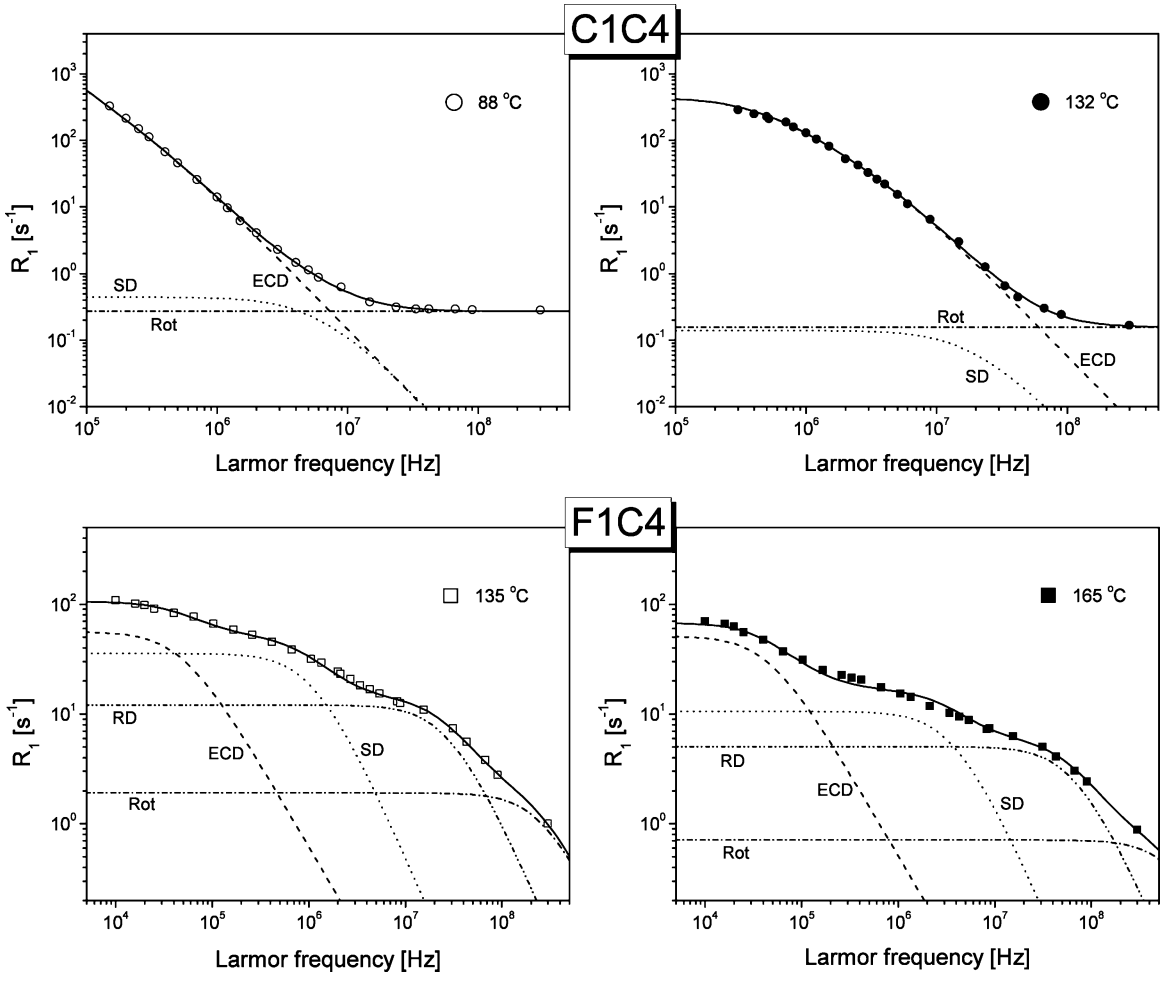

Figure 5. Fit of the R_1 dispersions in the Col_h phase at two temperatures for C1C4 and F1C4. The solid curve corresponds to the total fitting curve given by eq 1, and the separate contributions for the proposed dynamic mechanisms are shown. The model fitting parameters are displayed in Table 1.

dx.doi.org/10.1021/jp206225t | J. Phys. Chem. B 2012, 116, 2339–2346

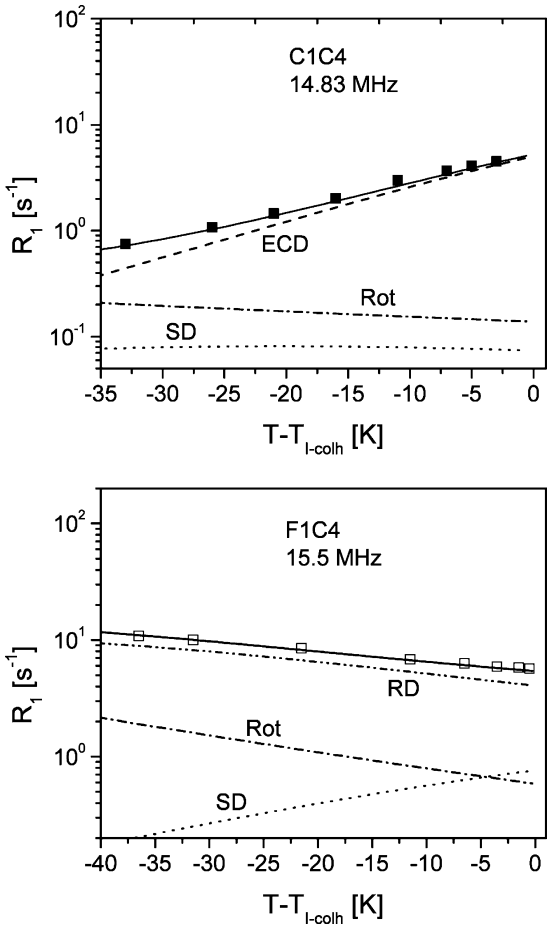

Figure 6. Fit of the temperature dependence of R_1 at 14.83 MHz for C1C4 and 15.5 MHz for F1C4 in the columnar phase. The contributions to the total relaxation rate from the different mechanisms are also displayed.

for a temperature in the middle of the columnar phase's temperature range[25] and Cruz et al. in C_8HET.[39] The corresponding activation energies (60 kJ/mol for F1C4 and 32 kJ/mol for C1C4) also show that the fluorination not only makes the translational diffusion motions slower and but also requires higher energy to activate this mechanism.

In what concerns the process of chain motion described by the BPP type function, correlation times ranging from 310 ps at 135 °C to 120 ps at 165 °C for F1C4 and from 2.8 ps at 88 °C to 1.6 ps at 132 °C for C1C4 were obtained. In the same trend as for the SD process, the chains' rotations show an activation energy higher for F1C4 than for C1C4: 49 and 15 kJ/mol, respectively. The prefactor A_{Rot} depends on the average interproton distance r ($A_{Rot} \propto 1/r^6$). Values r = 2.0 Å for F1C4 and r = 1.9 Å for C1C4 were obtained.

The large contribution of columns' undulations in C1C4 mask the process of rotations around the columnar axis in the NMRD. In F1C4, this relaxation mechanism is more influent than in the case of C1C4. The activation energy obtained for this process is 43 kJ/mol. This value is lower than 67 kJ/mol found by Dong et al. from the quadrupolar splitting and spin−lattice relaxation times T_{1Z} and T_{1Q} in a ring-deuterated 1-fluoro-2,3,6,7,10,11-hexahexyloxytriphenylene (F-HAT6).[43] The corresponding correlation times are in the ns scale in the whole range of the Col_h phase, in good agreement with the values obtained in ref 43.

These findings reflect the fact that in the columnar phase the effect of the fluorines in the chain ends is to slow down the chain motions and to make the intracolumn diffusion prevail over the intercolumn diffusion.

Isotropic Phase. In the isotropic phase, the partially fluorinated and the fully protonated molecules do not show major differences. Here, we discuss only the results in the F1C4. A first difference between the Col_h and Iso phases was found in the time recovery of the longitudinal magnetization in the whole frequency range measured here. While it was found to be monoexponential in the Col_h phase, a biexponential behavior was found in the isotropic phase. A monoexponential decay has been commonly observed not only the isotropic phase of rodlike thermotropic liquid crystalline samples[49,50] but also in the isotropic phase of the disk-like molecules.[39] There are examples of multiexponential behavior in the isotropic phase of other liquid crystals.[51−53] The two relaxation rates, R_{11} and R_{12}, obtained for both F1C4 and C1C4 samples were attributed to the aromatic moiety and to the aliphatic chains, respectively (see Figure 1).

At 15.5 MHz, in the isotropic phase, both relaxation rates increase slightly when the temperature decreases, but at 40 kHz, one of them increases more rapidly than the other one (see Figures 3 and 8).

The main difference with the Col_h phase is that R_1 dispersion in the isotropic phase is described only by individual molecular motions like rotations and translational diffusion.

In order to explain the results in the isotropic phase, the relaxation mechanisms considered were the following:

(i) Rotational reorientations of part or of the whole molecule, described by a single BPP contribution, as in the case of the Col_h phase. This includes rotations and/or molecular tumbling.

(ii) Molecular translational diffusion. Here, the model used was developed by Torrey for isotropic liquids and depends, basically, on the density of spins, n, the mean square jump distance, the intermolecular distance, d, and the correlation time τ_D.[54]

These processes are assumed to be Arrhenius like thermally activated.

(iii) Pretransitional effects, due to order parameter fluctuations (OPF), can appear close to the Iso−Col_h transition due to onset of local columnar order. A model for this contribution can be obtained starting from the Landau expansion of the free energy in terms of the local order parameter Ψ as

$$f = f_o + \frac{1}{2}A(T)\Psi^2 + \frac{1}{2}L_{\|}(\nabla_z\Psi)^2 + \frac{1}{2}L_{\perp}(\nabla_{\perp}\Psi)^2 \quad (3)$$

Here, f_o represents the free density energy in the isotropic phase without local fluctuations. $A(T) = a(T - T_c^*)$, T_c^* is a temperature slightly lower than the transition temperature ($T_c - T_c^* \sim 2$ K), a is a temperature independent constant, and $L_{\|}$ and $L_{\perp}$ are elastic moduli. The above expansion (eq 3) is valid if the order parameter is small. More details about the Landau expansion applied to liquid crystals can be found in refs 55 and 56.

Briefly, in terms of the wave vector $\mathbf{q}$, the damping time for each fluctuation in $\mathbf{q}$ is

$$\tau_{\mathbf{q}} = \frac{\eta}{A + \frac{1}{2}L_{\|}q_{\|}^2 + \frac{1}{2}L_{\perp}q_{\perp}^2}$$

dx.doi.org/10.1021/jp206225t | J. Phys. Chem. B 2012, 116, 2339−2346

where η is the effective viscosity. Using the usual procedure, the spectral density for the order parameter fluctuations (OPF) can be calculated as[56]

$$J_{\mathrm{OPF}}(\omega) = C \int_{q_{\perp,\min}}^{q_{\perp,\max}} \int_{q_{\parallel,\min}}^{q_{\parallel,\max}} \frac{q_\perp \, \mathrm{d}q_\perp \, \mathrm{d}q_\parallel}{\omega^2 + \frac{1}{\eta^2}(A + L_\parallel {q_\parallel}^2 + L_\perp {q_\perp}^2)^2}$$

The limits in the integrals are related to the minimum and the maximum wave vectors,[56] and C is a constant related with the visco-elastic properties of the liquid crystal in the isotropic phase.

The total experimental relaxation rate R_{1i} $(i = 1, 2)$ can be written as the sum of different contributions as

$$R_{1i} = R_{1i,\mathrm{OPF}} + R_{1i,\mathrm{Rot}} + R_{1i,\mathrm{SD}} + R_{1i,\mathrm{Tumb}}$$

assuming that each contribution is statistically independent of the others.

Following the same procedure used to analyze the data in the $\mathrm{Col_h}$ phase, a simultaneous model fit of the temperature and frequency dependences of the experimental R_{11} and R_{12} data was performed. The best fits are presented in Figures 7 and 8.

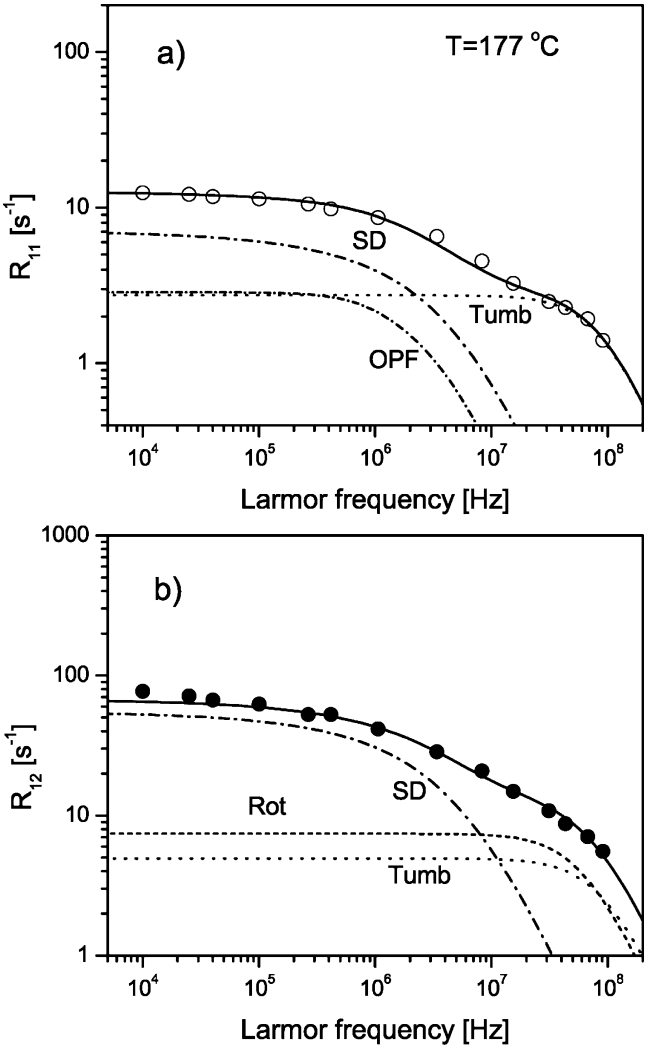

Figure 7. Fit of the relaxation rates frequency dispersion at 177 °C in the isotropic phase of F1C4: (a) R_{11} and (b) R_{12}. The contributions to the total relaxation rate from the different mechanisms are also displayed.

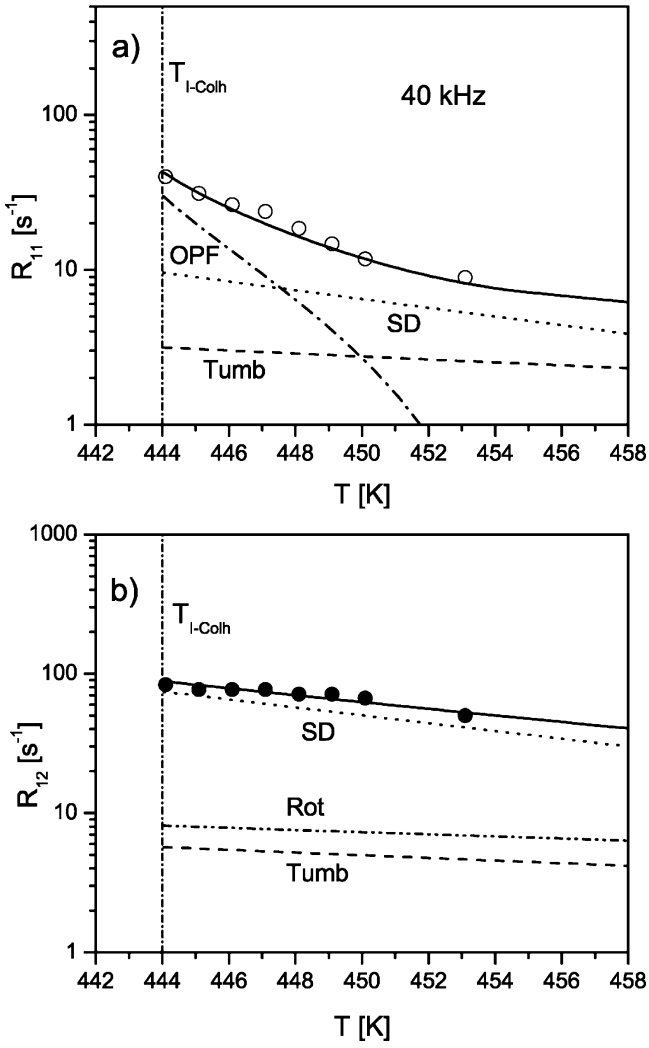

Figure 8. Fit of the temperature dependence of R_1 at 40 kHz in the isotropic phase of F1C4: (a) R_{11} and (b) R_{12}. The contributions to the total relaxation rate from the different mechanisms are also displayed.

Both relaxation rate components are interpreted in terms of the common relaxation mechanisms: self-diffsion (SD) and the whole molecular tumbling (Tumb). From the strength of the contribution of translation diffusion SD, a molecular jump distance average of 3.6 Å was obtained. This value is smaller than the 5.6 Å found in ref 25. The correlation time of the tumbling of the whole molecule is $\tau_t = \tau_{t,\infty} \exp(E_t/RT)$, with $\tau_{t,\infty} = 4.4 \times 10^{-14}$ s and E_t =37 kJ/mol.

Besides SD and Tumb, a full description of the data is accomplished with the help of the mechanisms Rot and OPF.

Comparing the temperature dependence of the R_{11} and R_{12} components (Figures 3 and 8), R_{11} presents a strong variation close to the transition only at low Larmor frequency (40 kHz). It reflects the pretransitional effects due to the formation columns close to the transition temperature. This means that the core is more sensitive than the chains to the onset of local columnar order. Figure 8a shows that OPF is the more efficient mechanism up to ~4 K above the phase transition. From the fit, it was found that T_c^* is 2 K lower than the clearing point.

In the case of the longest relaxation rate R_{12}, the free motion of the chains contribute also to the total relaxation rate. The correlation time corresponding to the rotation/reorientation

dx.doi.org/10.1021/jp206225t | J. Phys. Chem. B 2012, 116, 2339–2346

motion (Rot) was found $\tau_r = \tau_{r,\infty} \exp(E_r/RT)$ with $\tau_{r,\infty} = 4.6 \times 10^{-13}$ s and E_r =30 kJ/mol. The activation energy is smaller than the corresponding to the chain motion in the Col_h phase revealing the freedom to move in that phase. In Figure 8b, the fit and the contributions of R_{12} at 40 kHz are displayed.

CONCLUSIONS

In this work we present the results of a proton NMRD study of the molecular dynamics in the isotropic and columnar phases of a discotic liquid crystal with partially fluorinated triphenylene disk-like molecules. In the 2,3,6,7,10,11-hexakis-(1*H*,1*H*,2*H*,-2*H*,3*H*,3*H*-perfluorobutyloxy)triphenylene molecule, the protons in the CH_3 group of the aliphatic chains were replaced by fluorine. For a direct comparison, the NMRD profiles of the fully protonated homologue were collected. The study shows that, in both phases, the molecular dynamics in the high and middle frequency regimes (above ~20 MHz) is described by local reorientations/rotations of the aliphatic chains and of the triphenylene core. These motions are characterized by thermally activated correlation times. The activation energies obtained in the partially fluorinated compound are higher than those corresponding to the fully protonated one. In the Col_h phase, the spin−lattice relaxation rate results obtained in the sub-megahertz range are interpreted in terms of the elastic deformation of the columns. The contribution of ECD is clearly predominant up to frequencies around 10 MHz for the fully protonated sample. In the case of F1C4, ECD only dominates the relaxation for frequencies below 100 kHz.

Besides the difference in the shape of the NMRD profiles between the two phases, in the isotropic phase a biexponential decay of the magnetization was found in both compounds, contrary to the columnar phase where one relaxation rate was observed. The relaxation rates in the isotropic phase are attributed to the core (R_{11}) and the aliphatic chains (R_{12}). From the data analysis of the F1C4, it was found that the core is more sensitive to the onset of the columnar order associated with the formation of the columns since its pretransitional effect is reflected in it strong temperature dependence close to the transition.

Our findings show that the effect of fluorine in the aliphatic chains of triphenylene molecules not only enhances the columnar mesophase stability but also forces the thermally activated molecular motions to require higher activation energies. These conclusions are in agreement with previous results where the transition enthalpies for the clearing in the perfluorohexane derivatives increase with the number of fluorines in the aliphatic chains.[21]

ASSOCIATED CONTENT

Supporting Information

This material is available free of charge via the Internet at http://pubs.acs.org.

AUTHOR INFORMATION

Corresponding Author

*E-mail: fvchavez@cii.fc.ul.pt.

Notes

The authors declare no competing financial interest.

ACKNOWLEDGMENTS

Funding of this work was provided by Fundação para a Ciencia e a Tecnologa (FCT).

REFERENCES

(1) Chandrasekhar, S.; Sadashiva, B. K.; Suresh, K. A. *Pramana* **1977**, *9*, 471−480.
(2) Destrade, C.; Mondon, M. C.; Malhete, J. *J. Phys. Supp. C3* **1979**, *40*, 17−21.
(3) Demus, D., Goodby, J. W., Gray, G. W., Spiess, H. W., Vill, V., Eds. *Handbook of liquid crystals*; Wiley-VCH: New York, 1998.
(4) Laschat, S.; Baro, A.; Steinke, N.; Giesselmann, F.; Hägele, C.; Scalia, G.; Juele, R.; Kapatsina, E.; Sauer, S.; Schreivogel, A.; Tosoni, M. *Angew. Chem., Int. Ed.* **2007**, *46*, 4832−4887.
(5) Pisula, W.; Zorn, M.; Chang, J. Y.; Mullen, K.; Zentel, R. *Macromol. Rapid Commun.* **2009**, *30*, 1179−1202.
(6) Shimizu, Y.; Oikawa, K.; Nakayama, K. I.; Guillon, D. *J. Mater. Chem.* **2007**, *17*, 4223−4229.
(7) Funahashi, M. *Polymer J.* **2009**, *41*, 459−469.
(8) Schmidt-Mende, L.; Fechtenkotter, A.; Mullen, K.; Moons, E.; Friend, R. H.; MacKenzie, J. D. *Science* **2001**, *293*, 1119−1122.
(9) Hori, T.; Miyake, Y.; Yamasaki, N.; Yoshida, H.; Fujii, A.; Shimizu, Y.; Ozaki, M. *Appl. Phys. Express* **2010**, *3*, 101602.
(10) O'Neill, M.; Kelly, S. M. *Adv. Mater.* **2011**, *23*, 566−584.
(11) Bredas, J. L.; Calbert, J. P.; da Silva, D. A.; Cornil, J. *Proc. Natl. Acad. Sci. U.S.A.* **2002**, *99*, 5804−5809.
(12) Feng, X. L.; Marcon, V.; Pisula, W.; Hansen, M. R.; Kirkpatrick, J.; Grozema, F.; Andrienko, D.; Kremer, K.; Mullen, K. *Nat. Mater.* **2009**, *8*, 421−426.
(13) McMahon, D. P.; Troisi, A. *ChemPhysChem* **2010**, *11*, 2067−2074.
(14) Lemaur, V.; Da Silva Filho, D. A.; Coropceanu, V.; Lehmann, M.; Geerts, Y.; Piris, J.; Debije, M. G.; Van de Craats, A. M.; Senthilkumar, K.; Siebbeles, L. D. A.; Warman, J. M.; Bredas, J. L.; Cornil, J. *J. Am. Chem. Soc.* **2004**, *126*, 3271−3279.
(15) Bushby, R. J.; Lozman, O. R. *Curr. Opin. Colloid Interface Sci.* **2002**, *6*, 569−578.
(16) Gearba, R. I.; Anokhin, D. V.; Bondar, A. I.; Bras, W.; Jahr, M.; Lehmann, M.; Ivanov, D. A. *Adv. Mater.* **2007**, *19*, 815−820.
(17) Adam, D.; Closs, F.; Frey, T.; Funhoff, D.; Haarer, D.; Schuhmacher, P.; Siemensmeyer, K. *Phys. Rev. Lett.* **1993**, *70*, 457−460.
(18) Adam, D.; Schuhmacher, P.; Simmerer, J.; Häussling, L.; K., S.; Etzbachi, K. H.; Ringsdorf, H.; Haarer, D. *Nature* **1994**, *371*, 141−143.
(19) Kumar, S. *Liq. Cryst.* **2004**, *31*, 1037−1059.
(20) Terasawa, N.; Monobe, H.; Kiyohara, K.; Shimizu, Y. *Chem. Commun.* **2003**, 1678−1679.
(21) Terasawa, N.; Monobe, H.; Kiyohara, K.; Shimizu, Y. *Chem. Lett.* **2003**, *32*, 214−215.
(22) Simmerer, J.; Glusen, B.; Paulus, W.; Kettner, A.; Schuhmacher, P.; Adam, D.; Etzbach, K. H.; Siemensmeyer, K.; Wendorff, J. H.; Ringsdorf, H.; Haarer, D. *Adv. Mater.* **1996**, *8*, 815−819.
(23) Dong, R. Y. *Nuclear Magnetic Resonance Spectroscopy of Liquid Crystals*; World Scientific: Singapore, 2010.
(24) Žumer, S.; Vilfan, M. *Mol. Cryst. Liq. Cryst.* **1981**, *70*, 39−56.
(25) Vilfan, M.; Lahajnar, G.; Rutar, V.; Blinc, R.; Topic, B.; Zann, A.; Dubois, J. C. *J. Chem. Phys.* **1981**, *75*, 5250−5255.
(26) Shen, X.; Dong, R. Y.; Boden, N.; Bushby, R. J.; Martin, P. S.; Wood, A. *J. Chem. Phys.* **1998**, *108*, 4324−4332.
(27) Leisen, J.; Werth, M.; Boeffel, C.; Spiess, H. W. *J. Chem. Phys.* **1992**, *97*, 3749−3759.
(28) Zhang, J.; Dong, R. Y. *Phys. Rev. E* **2006**, *73*, 061704.
(29) Zhang, J.; Dong, R. Y. *J. Phys. Chem. B* **2006**, *110*, 15075−15079.
(30) Dong, R. Y.; Morcombe, R. C. *Liq. Cryst.* **2000**, *27*, 897−900.
(31) Werth, M.; Leisen, J.; Boeffel, C.; Dong, R. Y.; Spiess, H. W. *J. Phys. II* **1993**, *3*, 53−67.
(32) Goldfarb, D.; Dong, R. Y.; Luz, Z.; Zimmermann, H. *Mol. Phys.* **1985**, *54*, 1185−1202.
(33) Goldfarb, D.; Luz, Z.; Zimmermann, H. *J. Phys. (Paris)* **1981**, *42*, 1303−1311.
(34) Fischbach, I.; Ebert, F.; Spiess, H. W.; Schnell, I. *ChemPhysChem* **2004**, *5*, 895−908.

(35) Zamir, S.; Spielberg, N.; Zimmermann, H.; Poupko, R.; Luz, Z. *Liq. Cryst.* **1995**, *18*, 781−786.
(36) Rutar, V.; Blinc, R.; Vilfan, M.; Zann, A.; Dubois, J. C. *J. Phys. (Paris)* **1982**, *43*, 761−765.
(37) Kimmich, R.; Anoardo, E. *Progr. NMR Spectrosc.* **2004**, *44*, 257−320.
(38) Sebastião, P. J.; Cruz, C.; Ribeiro, A. C. In *Nuclear Magnetic Resonance Spectroscopy of Liquid Crystals*; Dong, R. Y., Ed.; World Scientific: Singapore, 2010; pp 129−167.
(39) Cruz, C.; Sebastião, P. J.; Figueirinhas, J. L.; Ribeiro, A. C.; Nguyen, H. T.; Destrade, C.; Noack, F. *Z. Naturforsch.* **1998**, *53a*, 823−827.
(40) Ribeiro, A. C.; Sebastião, P. J.; Cruz, C. *Pramana-J. Phys.* **2003**, *61*, 205−218.
(41) Liu, H.; Nohira, H. *Liq. Cryst.* **1997**, *22*, 217−222.
(42) Doi, T.; Sakurai, Y.; Tamatani, A.; Takenaka, S.; Kusabayashi, S.; Nishihata, Y.; Terauchi, H. *J. Mat. Chem.* **1991**, *1*, 169−173.
(43) Dong, R. Y.; Boden, N.; Bushby, R. J.; Martin, P. S. *Mol. Phys.* **1999**, *97*, 1165−1171.
(44) Dahn, U.; Erdelen, C.; Ringdorf, H.; Festag, R.; Wendorff, J. H.; Heiney, P. A.; Maliszewskyj, N. C. *Liq. Cryst.* **1995**, *19*, 759−764.
(45) Sousa, D.; Domingos Marques, G.; Cascais, J. M.; Sebastião, P. J. *Solid State NMR* **2010**, *38*, 36−43.
(46) Levelut, A. M. *J. Phys., Lett.* **1979**, *40*, L81−L84.
(47) Bloembergen, N.; Purcell, E. M.; Pound, R. V. *Phys. Rev.* **1948**, *73*, 679−712.
(48) http://fitter.ist.utl.pt. Online software for curve fitting using user-defined functions.
(49) Vaca Chávez, F.; Acosta, R. H.; Pusiol, D. J. *Chem. Phys. Lett.* **2004**, *392*, 403−408.
(50) Vaca Chávez, F.; Bonetto, F.; Pusiol, D. J. *Chem. Phys. Lett.* **2000**, *330*, 368−372.
(51) Apih, T.; Domenici, V.; Gradišek, A.; Hamplová, V.; Kaspar, M.; Sebastião, P. J.; Vilfan, M. *J. Phys. Chem. B* **2010**, *114*, 11993−12001.
(52) Grande, S.; Heinze, E.; Losche, A. *Phys. Lett. A* **1976**, *58*, 102−104.
(53) Hayward, R. J.; Packer, K. J. *Mol. Phys.* **1973**, *25*, 1443−1450.
(54) Torrey, H. C. *Phys. Rev.* **1953**, *92*, 962−969.
(55) DeGennes, P. G.; Prost, J. *The Physics of Liquid Crystals*, 2nd ed.; Clarendon Press: Oxford, 1993.
(56) Dong, R. *Nuclear Magnetic Resonance of Liquid Crystals*, 2nd ed.; Springer-Verlag: New York, 1997.